Supporting Information

Table S1. Affinity of various gp120 ligands to WT and E275C YU-2 gp120 assessed using SPR. Corresponding sensorgrams are shown in Figures S12-S14.

Analyte	K_D (nM)	
	WT	E275C
sCD4	2.20	24.0
17b	18.0	44.5
b12	28.0	21.0

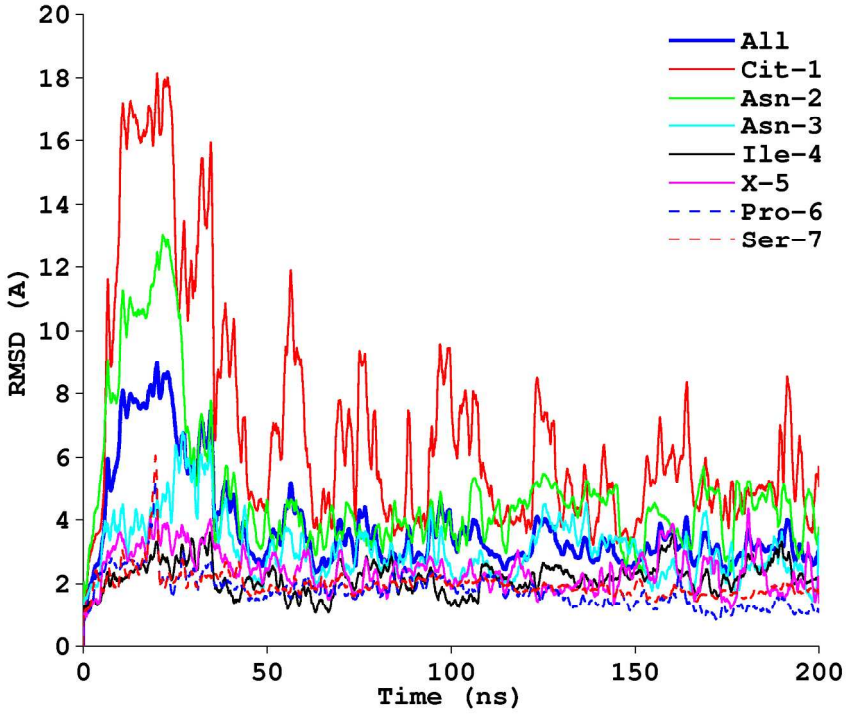

Figure S1. Heavy atom RMSD trace for various peptide residues during 200 ns of explicit-solvent all-atom MD equilibration of the minimum energy peptide triazole (UM101)/gp120 encounter complex. "X-5" denotes the derivatized azidoproline. The RMSD for all peptide residues is plotted in thick blue.

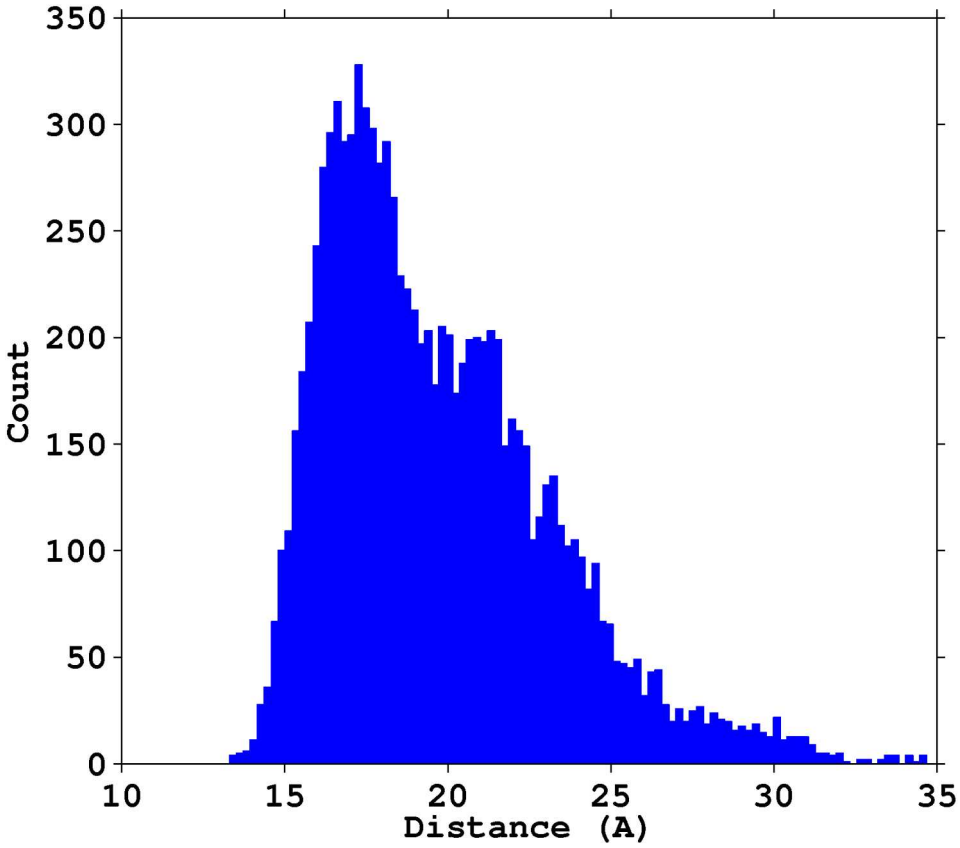

Figure S2. Frequency count for distance of the peptide backbone N-terminal nitrogen to gp120 E275 (C_γ atom of the side chain) throughout the 200 ns equilibration trajectory reported in this study. The data were grouped into 100 discrete bins. Mean = 19.73 Å; Mode = 17.41 Å.

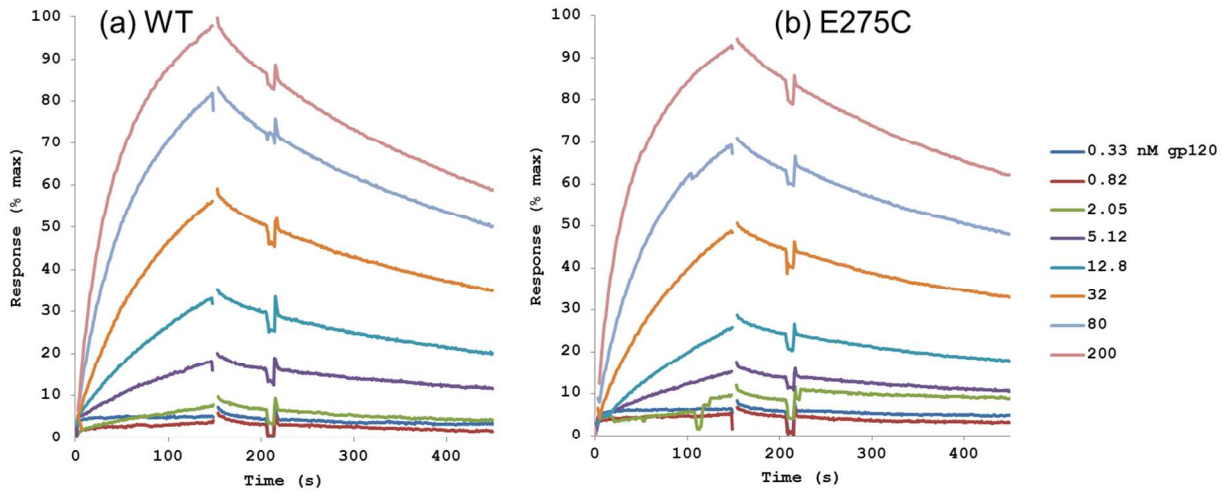

Figure S3. SPR sensorgrams for direct binding of **(a)** WT **(b)** E275C gp120 to a peptide triazole variant (SR07C) immobilized on the SPR chip surface. Numbers on the right show the gp120 concentrations in nM.

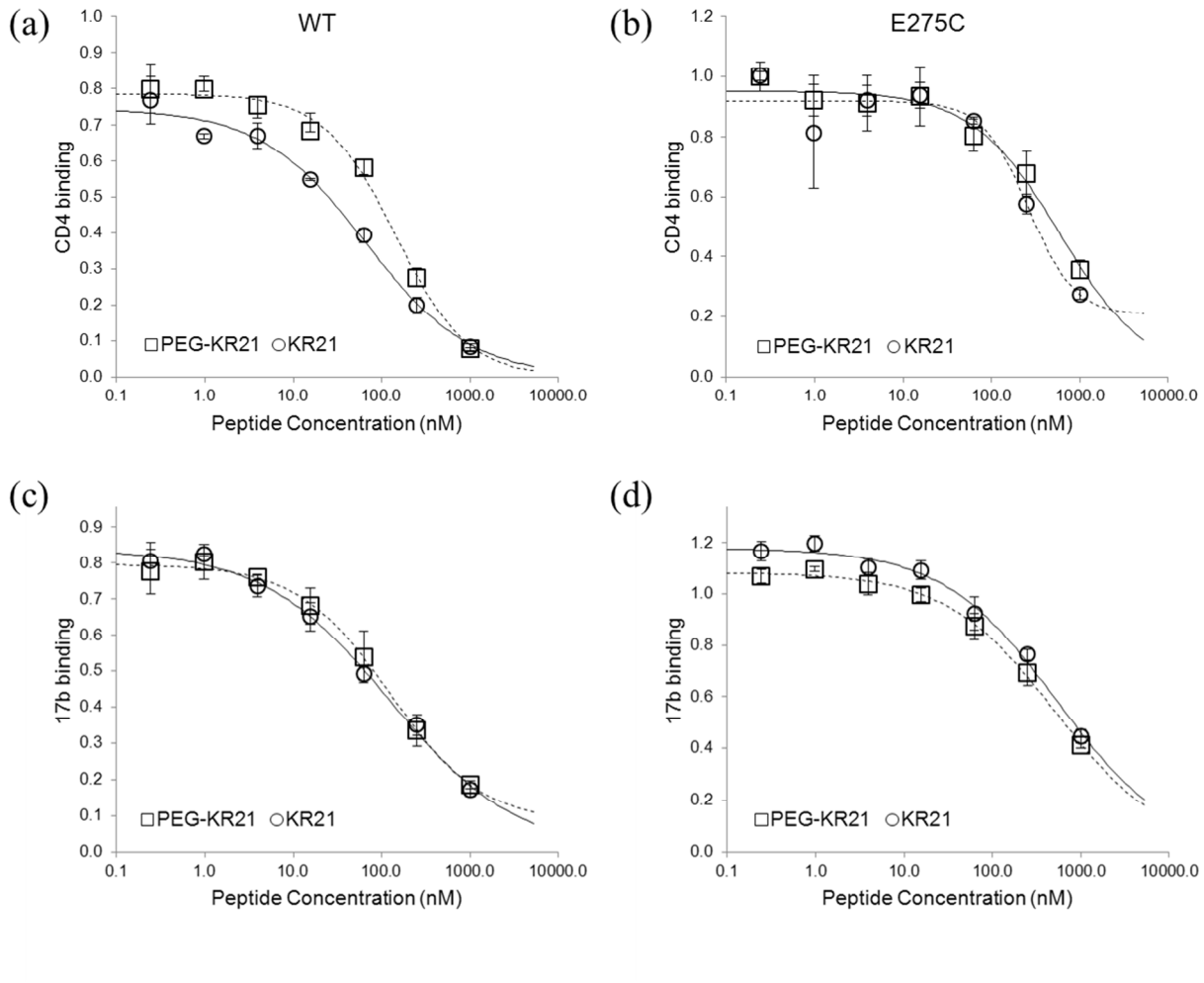

(e)

	WT_{IC50}		$E275C_{IC50}$	
Peptide	sCD4	17b	sCD4	17b
KR21	66	122	262	520
PEG-KR21	144	123	599	502

Figure S4. Competition ELISA for inhibition of binding of **(a)** sCD4 to WT gp120 **(b)** sCD4 to E275C **(c)**mAb 17b to WT and **(d)**mAb 17b to E275C gp120 by KR21 (circles) or PEG-KR21 (squares). Error bars represent standard deviations (n=2). The data were fitted to a logistic curve and the results are provided as guide to the eye (solid lines for KR21 and dashed lines for PEG-KR21). **(e)** Approximate IC_{50} values from the fits shown in panels **a-d**.

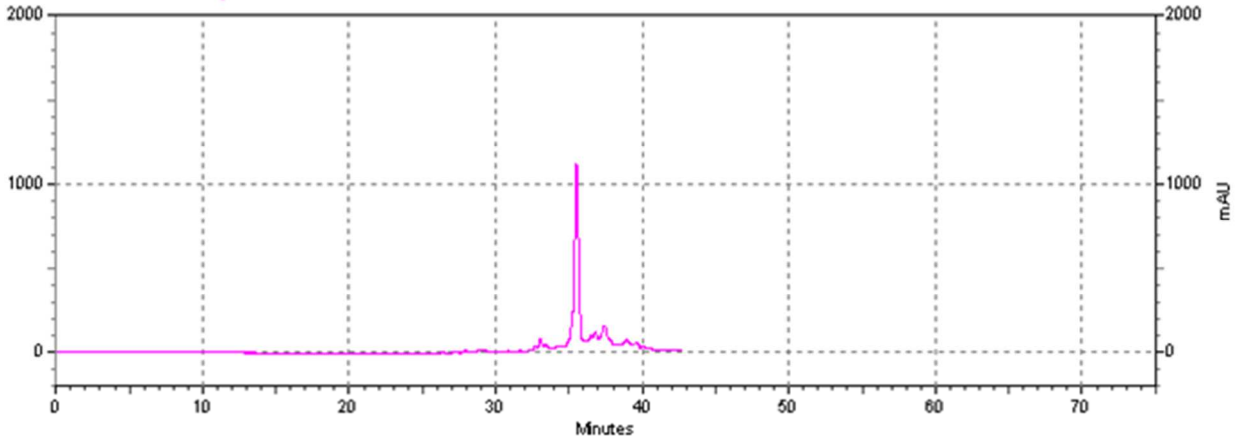

Figure S5. SR07C HPLC chromatogram.

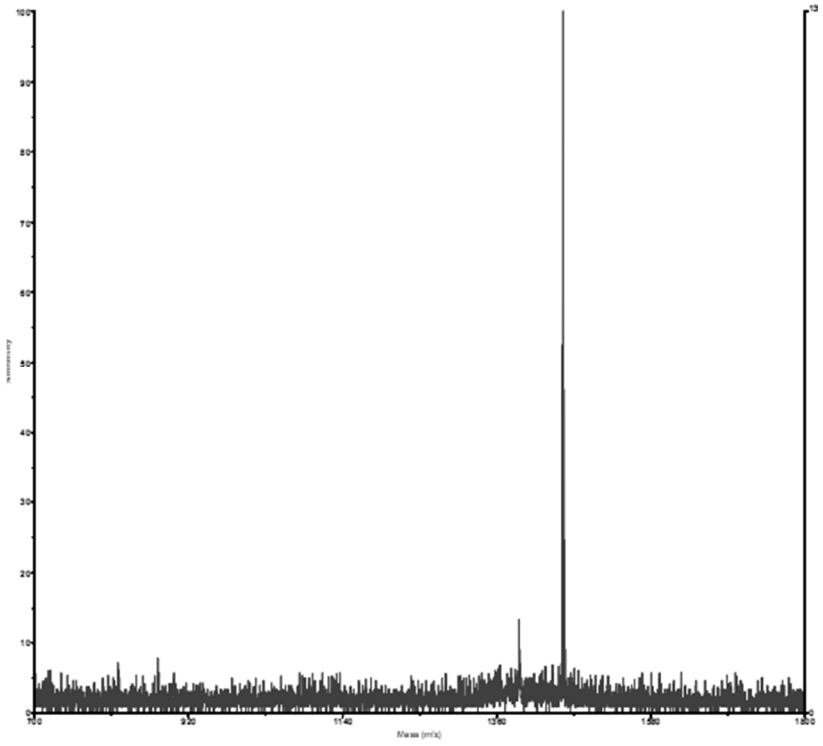

Figure S6. TOF MS results for SR07C. Observed MW=1453.5 Da, Expected MW=1453.8 Da.

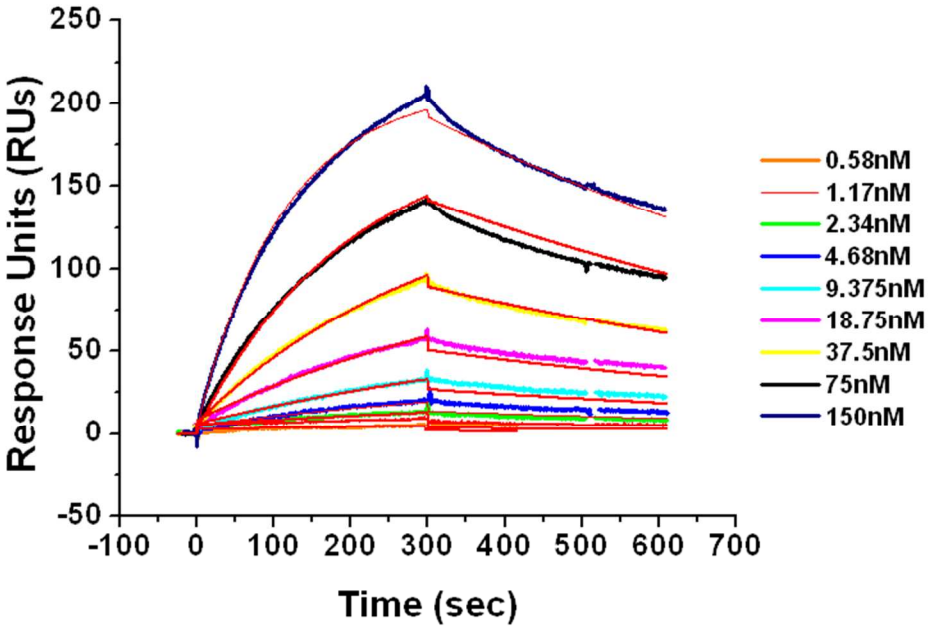

Figure S7. SPR sensorgram for determining SR07C affinity to gp120YU-2. Different concentrations of the latter (indicated in the figure inset) were passed over 23.2 RUs of SR07C surface-immobilized through the peptide C-terminal thiol. Curves were fit to a global 1:1 kinetic model and the results of the fit are shown in red overlay lines. K_D= 23.9 nM.

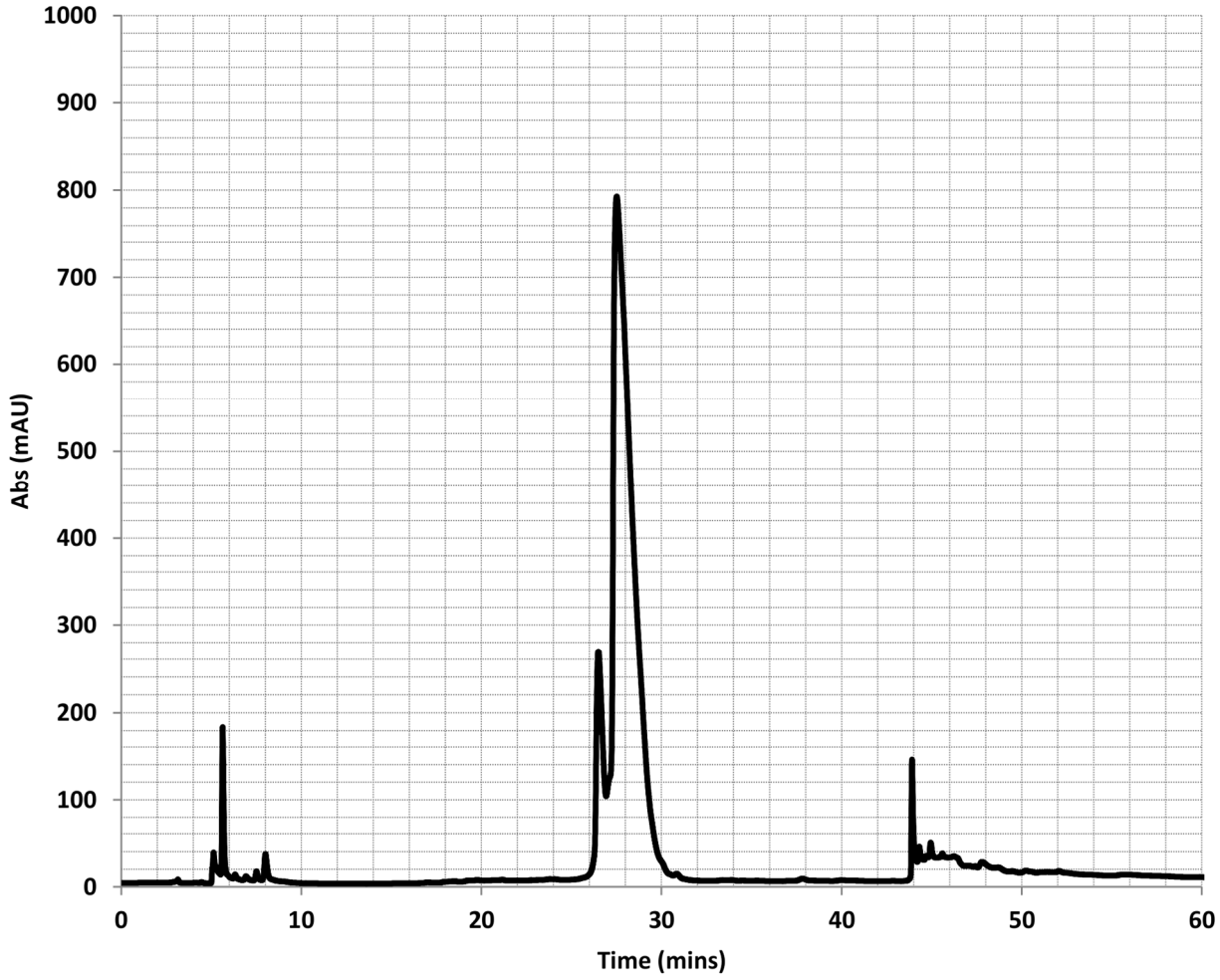

Figure S8. PEG-KR21 RP HPLC chromatogram

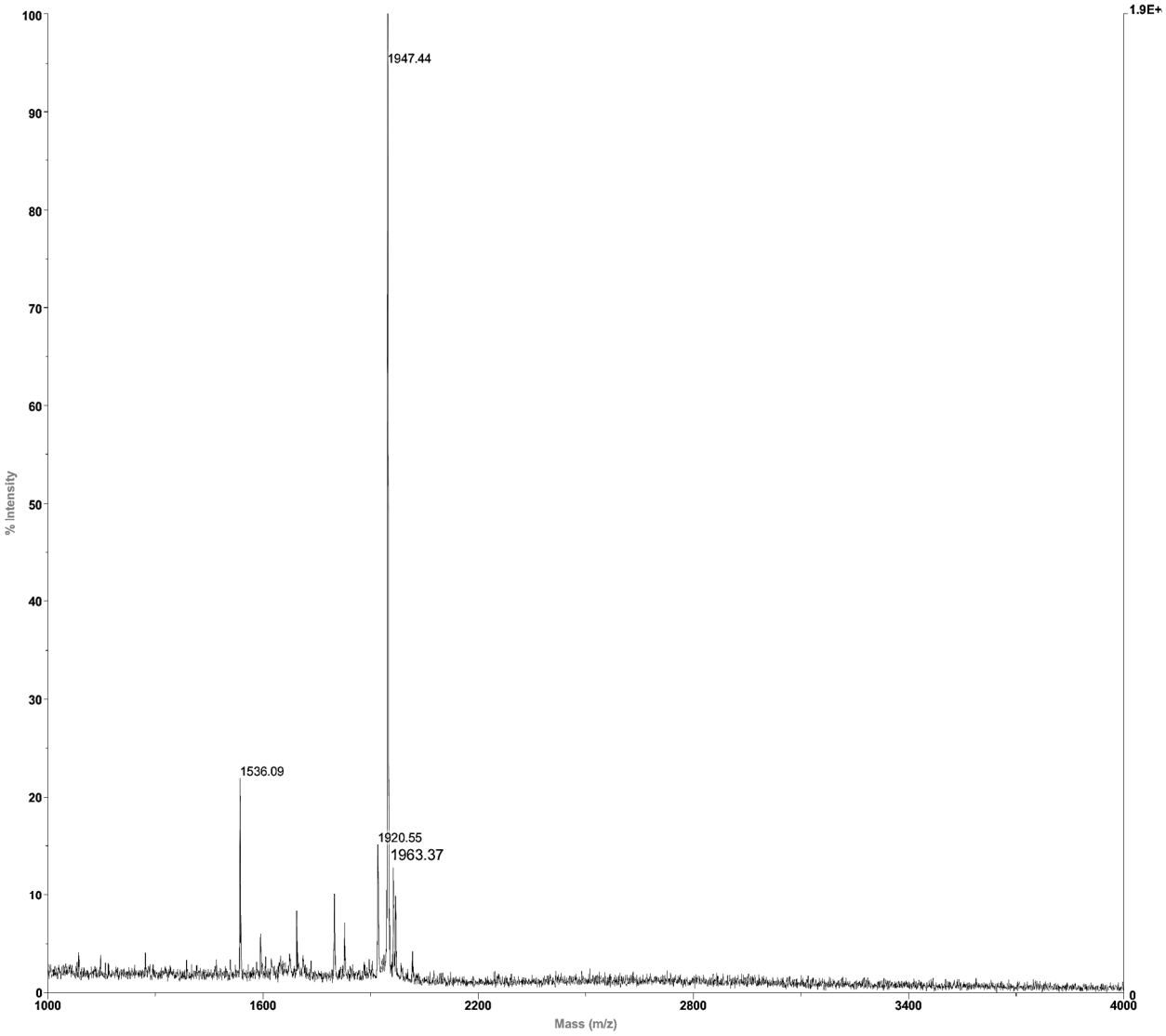

Figure S9. MALDI TOF MS results for PEG-KR21. Observed MW=1947.44 Da, Expected MW=1946.1 Da.

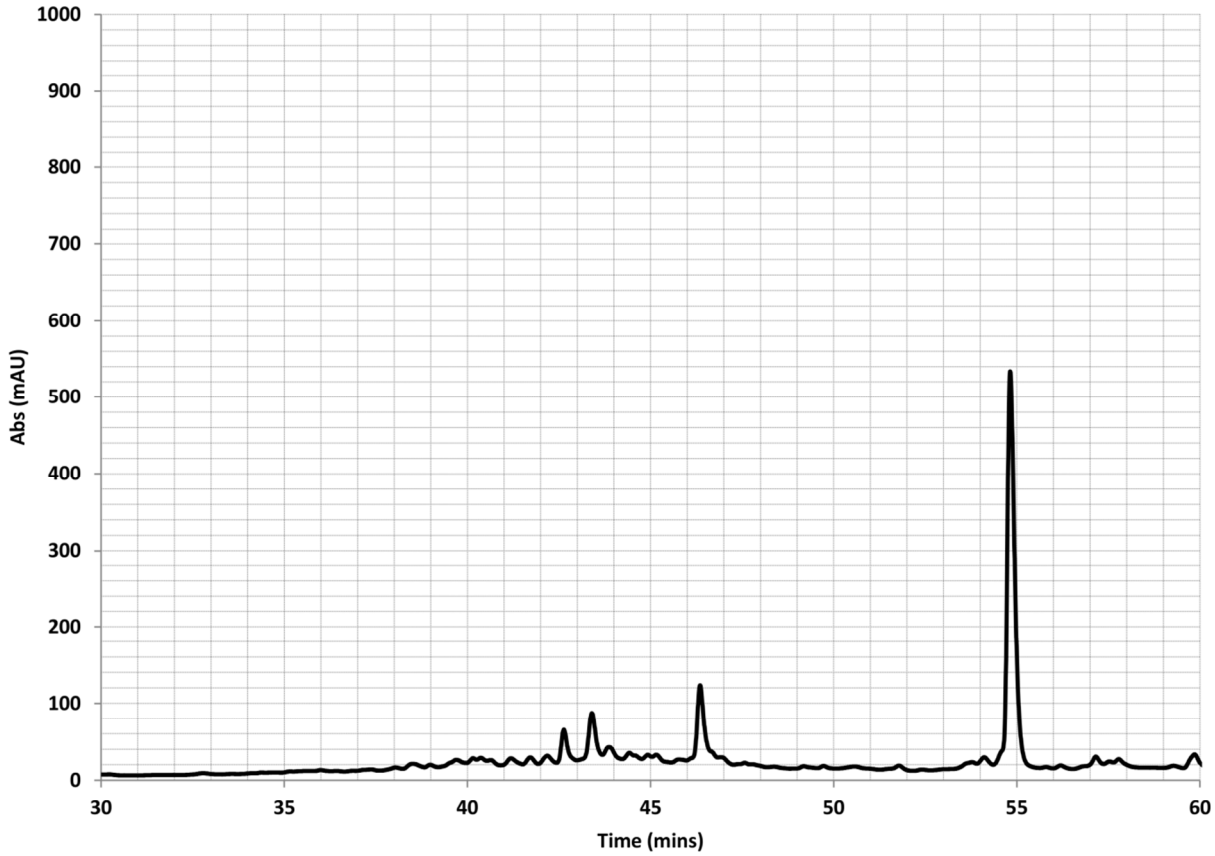

Figure S10. AE21 RP HPLC chromatogram

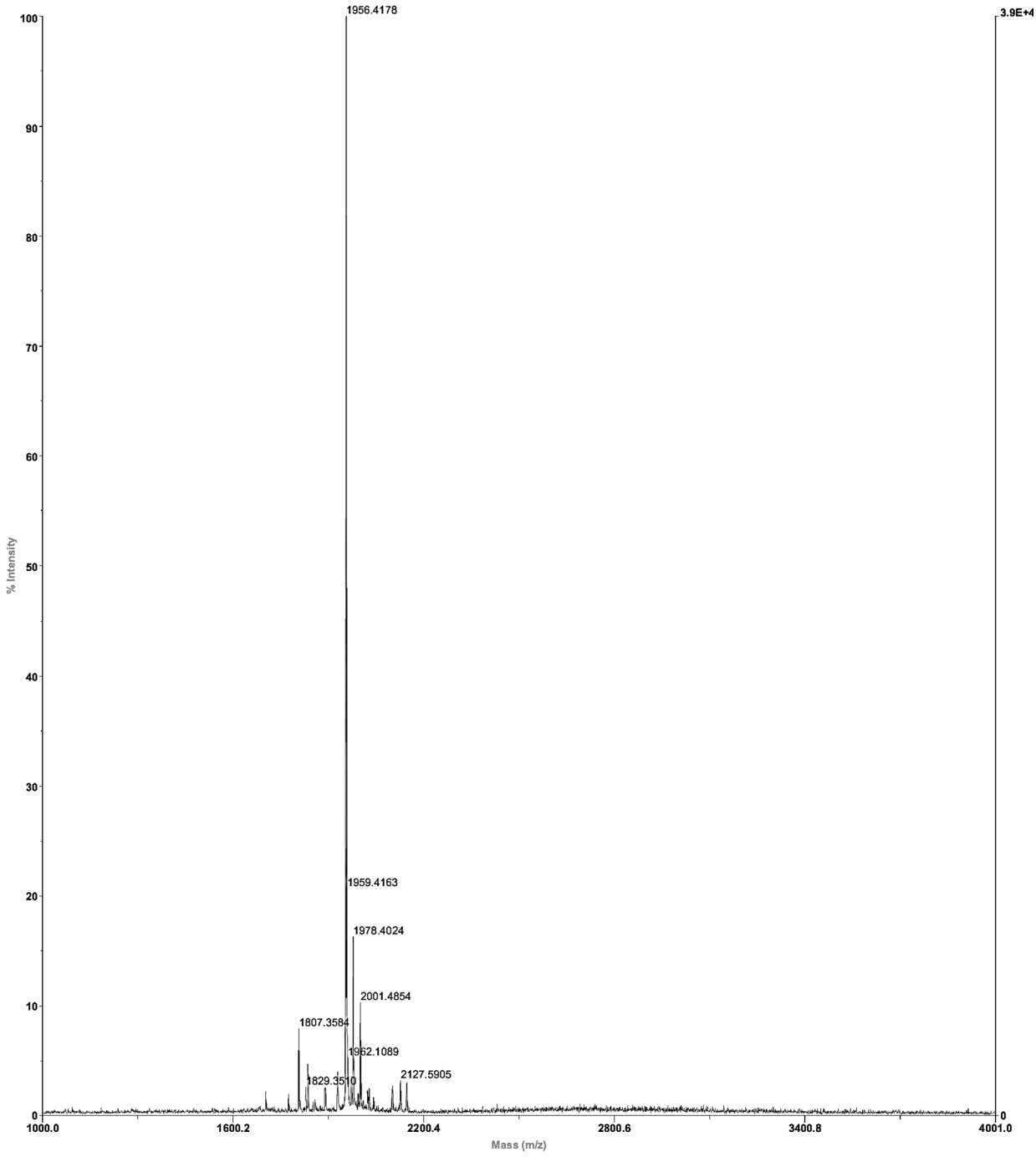

Figure S11. MALDI TOF analysis of AE21. Observed MW=1956.42 Da, Expected MW=1954 Da.

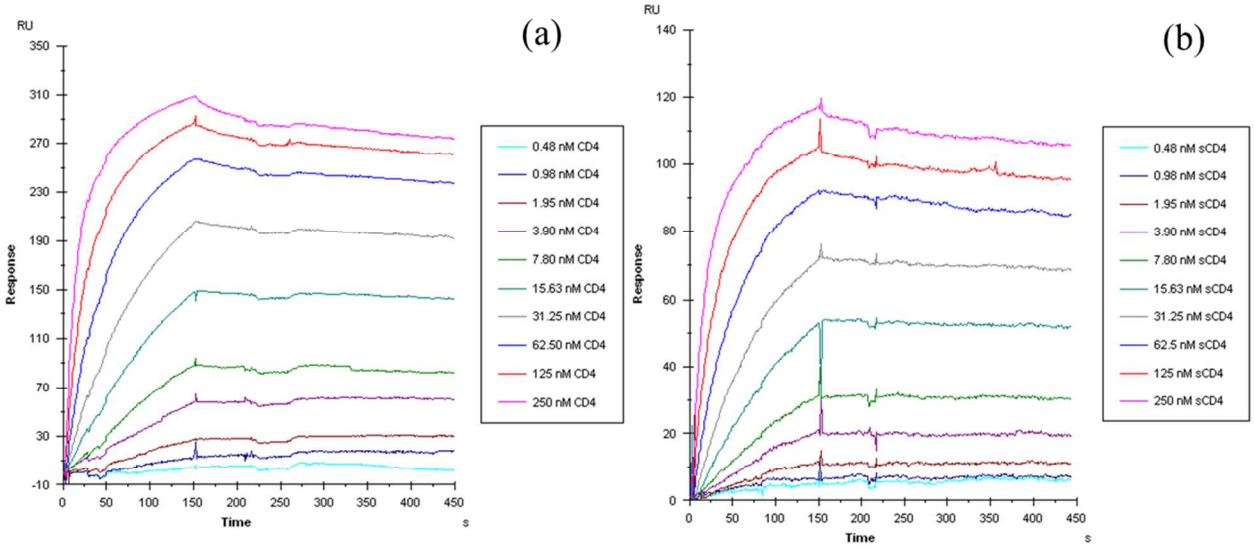

Figure S12. SPR sensorgrams for direct binding of sCD4 to immobilized **(a)** WT **(b)** E275C $gp120_{YU-2}$. Numbers on the right show analyte concentrations (n=2).

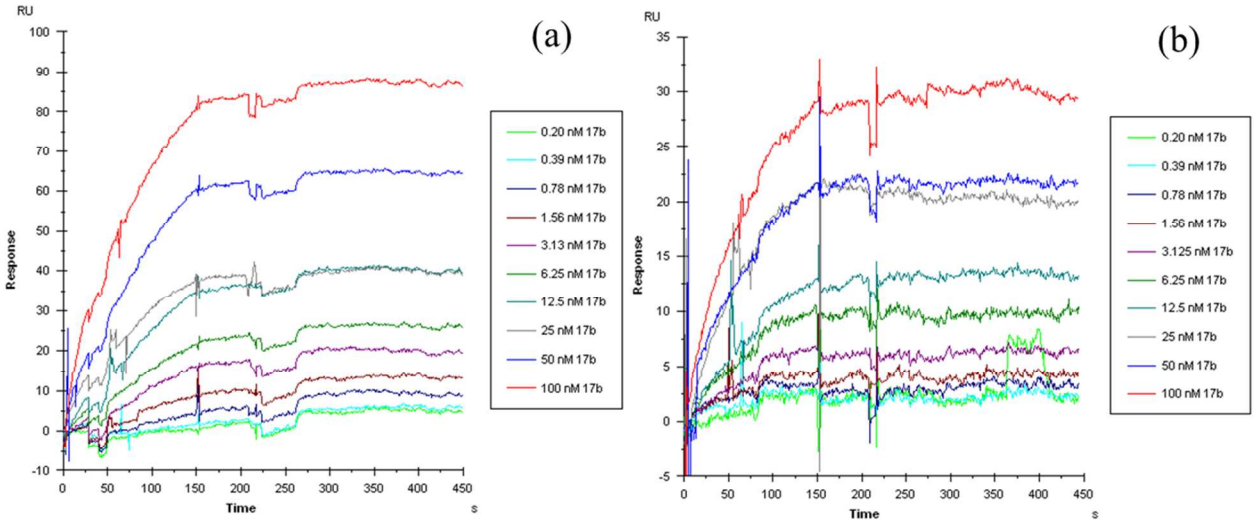

Figure S13. SPR sensorgrams for direct binding of mAb 17b to immobilized **(a)** WT **(b)** E275C $gp120_{YU-2}$. Numbers on the right show analyte concentrations (n=2).

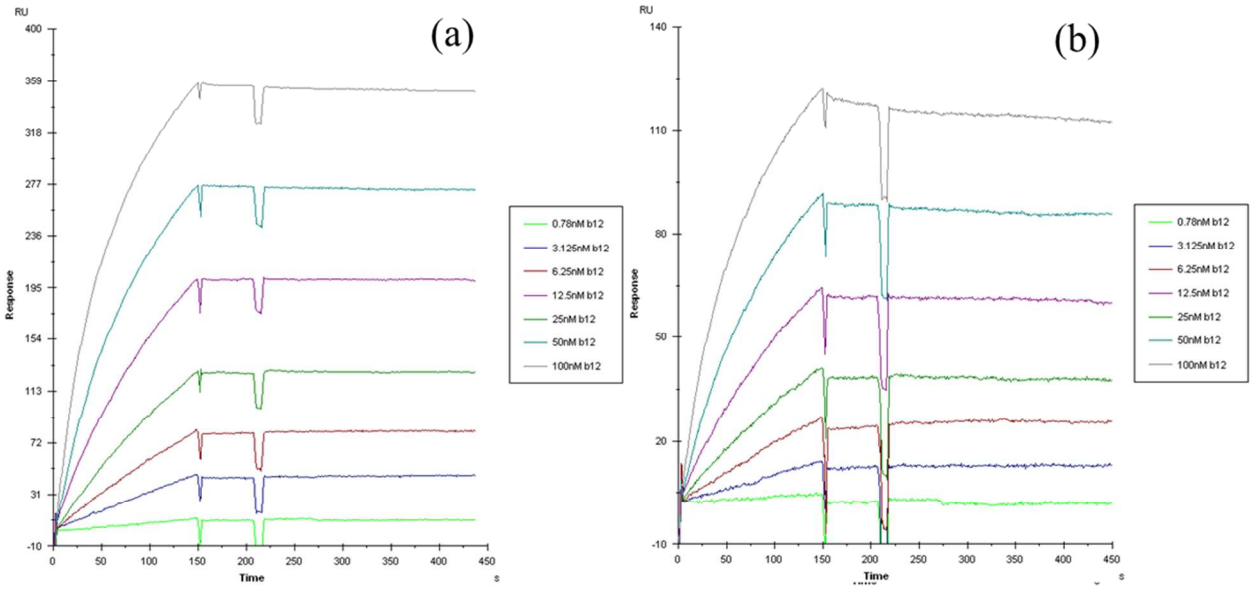

Figure S14. SPR sensorgrams for direct binding of mAb b12 to immobilized **(a)** WT **(b)** E275C $gp120_{YU-2}$. Numbers on the right show analyte concentrations (n=2).